Article

Subtype- and race-specific variations in the immune landscape of breast cancer: therapeutic implications

Check for updates

Amod Sharma[1,2], Sarabjeet Kour Sudan[1,2], Kunwar Somesh Vikramdeo[1,2], Mohammad Aslam Khan[3,4,6], Muhammad Tahir[3], James E. Carter[3], Todd Kendall[5], Cindy Nelson[4], Ajay P. Singh[1,2] & Seema Singh[1,2] ✉

Breast cancer is a heterogeneous disease with distinct molecular subtypes that disproportionately affects Black women. Immune cells are a key component of the tumor microenvironment, influencing tumor growth and treatment outcomes. Here, we explored immune landscape differences between TNBC and non-TNBC subtypes, assessing any race-specific patterns. TNBC showed higher infiltration of B-cells, Treg cells, Th1 cells, and CD8+ cells, and fewer mast cells than non-TNBC. Race-wise comparisons revealed that White TNBC had more Th1 cells than Black TNBC, while Black non-TNBC exhibited higher NK and Treg cells but lower DCs. KEGG pathway analysis identified immunosuppression in TNBC, with Black patients exhibiting the same regardless of molecular subtype. Higher TAM and lower T-cell infiltration were linked to metastatic disease. In White patients, lower immune cells (particularly T-cells, DCs, and NK cells) correlated with more metastasis, but not in Black patients. These race- and subtype-specific immune differences may guide tailored immunotherapies.

Breast cancer (BC) is the most frequently diagnosed malignancy in women worldwide[1]. Approximately 316,950 women will be diagnosed with BC this year in the United States alone, and nearly 42,170 will succumb to the disease[2]. At the molecular level, BC is broadly classified into four molecular subtypes, luminal A [estrogen and progesterone receptor positive (HR+), human epidermal growth factor receptor 2 negative (HER2−)], luminal B (HR+ HER2−/+ with high Ki67), HER2 enriched (HR− HER2+), and triple-negative breast cancer (TNBC or HR- HER2−)[3,4]. Among these, luminal subtypes have the best prognosis, followed by the HER2-enriched subtype due to the availability of targeted therapies. TNBC has the worst prognosis because of its highly aggressive nature and limited availability of effective therapeutic options[5,6].

Significant health disparities are observed in patients diagnosed with BC; especially Black women appear to bear the greatest burden. Although the BC death rate has declined by approximately 44% over the past decade, it has remained largely unchanged in Black women for the past several decades. Black women experience 38% higher mortality compared to their White counterparts despite having a 5% lower incidence rate[6,7]. Moreover, they are diagnosed with BC at a younger age and have nearly twice the

frequency of diagnosis with the TNBC subtype compared to White women[8,9]. Black women diagnosed with the luminal subtype are also more likely to relapse after endocrine therapy, further adding to their elevated mortality rates[10]. Clearly, there is a critical need to deepen our understanding of the molecular pathobiology of BC and develop new mechanism-based therapies to improve its clinical management and address existing disparities.

Immune system-targeted therapies have gained high prominence in recent years and have shown great promise for the clinical management of various cancers[11–13]. Immune cells are a crucial component of the tumor microenvironment (TME) that play a significant role in tumor development and therapeutic outcomes[14,15]. Cancer and other stromal cells residing in TME modulate the immune cell infiltration and their functional phenotypes in a way that creates an immunosuppressive microenvironment, helping the tumor cells evade immune killing. Understanding these aspects can help develop insights into BC pathobiology and holds promise for immune therapeutic management. In the present study, we analyzed the immune landscape of breast tumors and compared the differences across race or BC molecular subtypes. We also determined the immune signaling pathways

[1]Department of Cell and Molecular Biology, University of Mississippi Medical Center, Jackson, MS, USA. [2]Cancer Center and Research Institute, University of Mississippi Medical Center, Jackson, MS, USA. [3]Department of Pathology, University of South Alabama, Mobile, AL, USA. [4]Mitchell Cancer Institute, University of South Alabama, Mobile, AL, USA. [5]Department of Pathology, Providence Hospital, University of South Alabama, Mobile, AL, USA. [6]Department of Pharmacy and Pharmaceutical Sciences, St. Jude Children's Research Hospital, Memphis, TN, USA. ✉e-mail: ssingh3@umc.edu

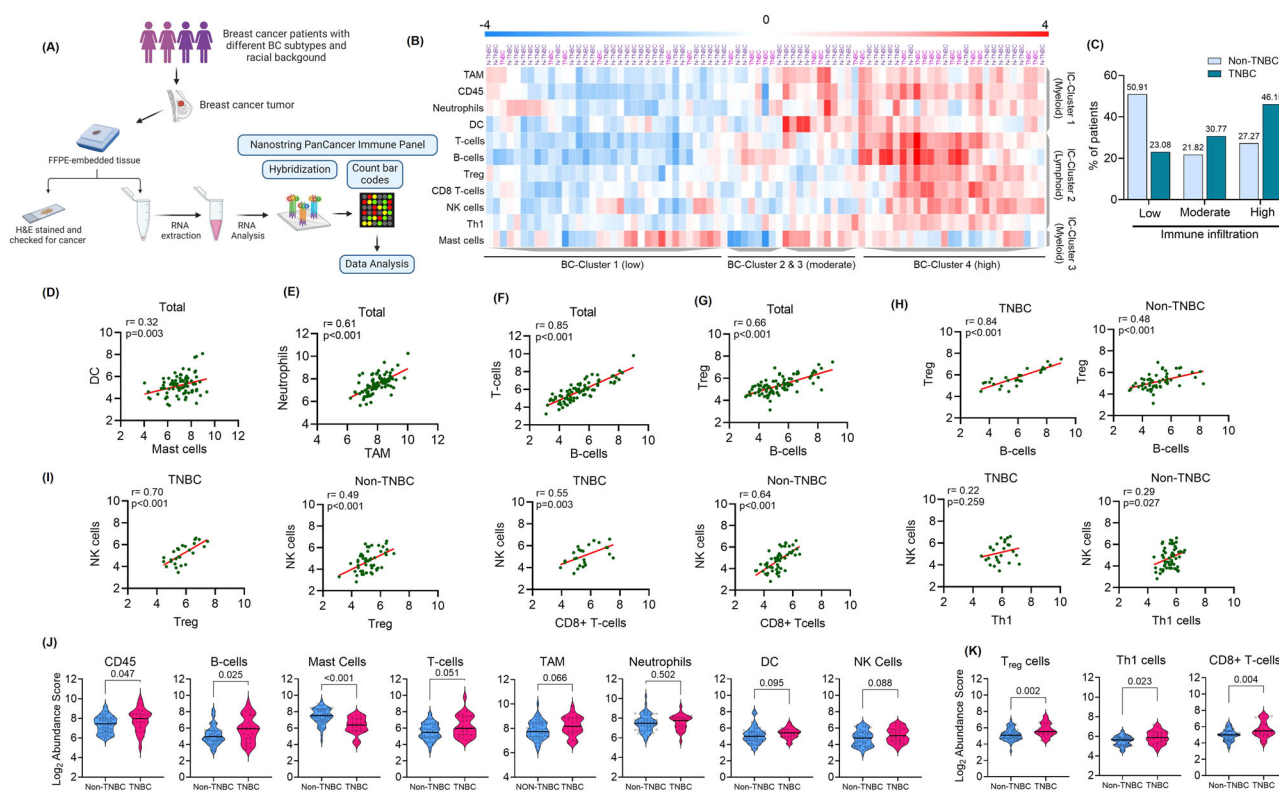BCRF BREAST CANCER RESEARCH FOUNDATION

that were differentially regulated in these tumors and explored the relationship between immune infiltration and tumor metastasis.

Results

TNBC and non-TNBC subtypes exhibit differential tumor immune microenvironment

To investigate the differences in the immune landscape between TNBC and non-TNBC molecular subtypes, we performed immune cell profiling on 81 BC tumor samples (55 non-TNBC and 26 TNBC) using the nanoString PanCancer immune panel on the nCounter® pro analysis system (Fig. 1A). The immune cell abundance score was determined for each sample by the Rosalind software based on average expression values of their corresponding marker genes. Unsupervised clustering based on the abundance score of different immune cell types grouped all the samples into four major clusters (BC Clusters 1–4) in the heat map, with Cluster 1 and Cluster 4 exhibiting low and high tumor-infiltrating lymphocytes (TILs), respectively, and Clusters 2 and 3 having moderate TILs (Fig. 1B). Immune cells were also clustered into three major clusters (IC-Clusters 1–3). IC-Cluster 1 consisted of cells of myeloid lineage, such as tumor-associated macrophages (TAMs), neutrophils, and dendritic cells (DC), except for mast cells, which were placed alone in IC-Cluster 3. All the immune cells of lymphoid lineage, like T-cells, B-cells, regulatory T-cells (Tregs), CD8+ T-cells, Th1 cells, and natural killer (NK) cells, were grouped in IC-Cluster 2 (Fig. 1B). Notably, the distribution of TNBC and non-TNBC samples within the BC-Clusters revealed that the moderate and high TILs clusters contained a higher percentage of TNBC, while a greater percentage of non-TNBC were placed in the low TILs cluster (Fig. 1C).

Since in our unsupervised clustering analysis, mast cells did not cluster with other cells of the myeloid lineage, we examined their correlative abundance with other immune cell types using the Pearson correlation analysis. A significant positive correlation ($r = 0.32$, $p = 0.003$) was observed with DC infiltration only (Fig. 1D) in both TNBC ($r = 0.40$, $p = 0.039$) and non-TNBC ($r = 0.45$, $p < 0.001$) (Fig. S1A). Among other cell types of myeloid origin, we observed the strongest significant correlation between TAM and neutrophils ($r = 0.61$, $p < 0.001$) (Fig. 1E) in both TNBC ($r = 0.66$, $p < 0.001$) and non-TNBC ($r = 0.60$, $p < 0.001$) (Fig. S1B). A significant positive correlation was also observed between TAM and DC ($r = 0.58$, $p < 0.001$) but not between DC and neutrophils ($r = 0.18$, $p = 0.099$) (Fig. S1C, D). Among lymphoid-origin immune cells, the highest significant correlation was observed between B-cells and T-cells ($r = 0.85$, $p < 0.001$) (Fig. 1F) in both TNBC ($r = 0.88$, $p < 0.001$) and non-TNBC ($r = 0.80$, $p < 0.001$) (Fig. S1E). Among the T cell subtypes, Tregs showed the highest correlation with B-cells ($r = 0.66$, $p < 0.001$) compared to Th1 ($r = 0.48$, $p < 0.001$) and CD8 + T-cells ($r = 0.57$, $p < 0.001$) (Figs. 1G and S1F), which was notably stronger in TNBC ($r = 0.84$, $p < 0.001$) than in non-TNBC ($r = 0.48$, $p < 0.001$) (Fig. 1H). Besides, NK cells correlated strongly with Tregs in TNBC, while they showed better correlations with CD8 + T-cells and Th1 cells in non-TNBC (Fig. 1I). In overall abundance score comparisons between TNBC and non-TNBC, a significantly higher ($p = 0.047$) presence of lymphocytes represented by CD45 positivity was observed in TNBC than in non-TNBC. TNBC also had significantly higher B-cell infiltration ($p = 0.025$) and a strong trend for higher T-cells ($p = 0.051$) and TAM ($p = 0.066$) infiltration as well; however, the mast cell infiltration was significantly lower in TNBC than in non-TNBC ($p < 0.001$) (Fig. 1J). Among

Fig. 1 | Distinct tumor immune microenvironments in TNBC and non-TNBC BC subtypes. A Graphical presentation of the working strategy used for immune cell abundance analysis in the tumor samples. B Heat map showing the unsupervised hierarchical clustering of immune cell types and TNBC and non-TNBC cases based on immune abundance scores and patterns. C Percentage distribution of TNBC and non-TNBC samples in low, moderate, and high immune infiltration clusters obtained from the heatmap. Scatter plot showing the Pearson correlation coefficient (r) of mast cells with DC (D), TAM with neutrophils (E), B-cells with T-cells (F), and B-cells with Treg cells (G) infiltration, calculated from the immune abundance scores across total samples. (H and I) Scatter plot showing the Pearson correlation coefficient (r) for infiltration of B-cells with Treg cells (H), NK cells with Treg cells, CD8+ T-cells, and Th1 cells, calculated from the immune abundance scores in TNBC and non-TNBC samples. Comparison of the immune abundance score among TNBC and non-TNBC samples for overall immune infiltration represented by CD45 positive cells, B-cell, mast cells, T-cells, TAM, neutrophils, DC, and NK cells (J), Treg cells, Th1 cells, and CD8+ T-cells (K). A non-parametric Mann–Whitney test was used to determine the p-value. A p-value < 0.05 was considered statistically significant.

T-cell subpopulations, Tregs ($p = 0.002$), Th1 cells ($p = 0.023$), and CD8+ T-cells ($p = 0.004$) infiltration was significantly higher in TNBC compared to non-TNBC (Fig. 1K). When we compared immune cell infiltration in non-TNBC subtypes between hormone receptor-positive (HR+) and hormone receptor-negative (HR−), HR− samples had a significantly higher Treg cell infiltration ($p = 0.010$) than HR+ samples (Fig. S1G).

Racial variations in the abundance of the TILs in TNBC and non-TNBC samples
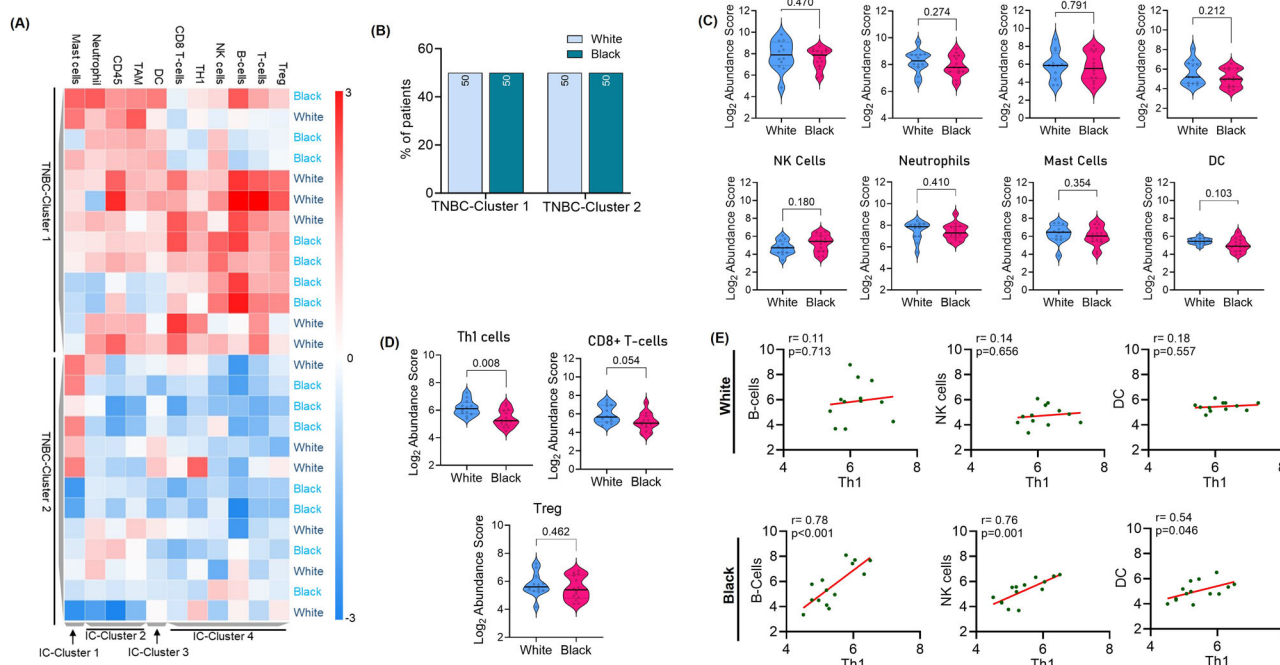
Next, we examined whether the pattern of immune cell infiltration in TNBC and non-TNBC subtypes varied between White and Black patients. For this, we performed the unsupervised clustering of TNBC cases from White and Black patients and examined the sample distribution in clusters with varying levels of TILs. Analysis created two distinct clusters of TNBC with relatively high TILs (TNBC-Cluster 1) and low TILs (TNBC-Cluster 2). The immune cells were clustered into four clusters (IC Clusters 1–4), with IC-Cluster 1 having Mast cells, IC-Cluster 2 having other myeloid cells, IC-Cluster 3 having DC, and IC-Cluster 4 having all other immune cells of lymphoid lineage (Fig. 2A). However, TNBC from Black and White patients showed equal distribution in both high and low TILs clusters (Fig. 2B). Moreover, we also did not observe significant differences in the immune cell abundance scores between the Black and White patients (Fig. 2C). Interestingly, among the T-cell subpopulations, we observed a significantly higher abundance of Th1 cells ($p = 0.008$) in White TNBC patients along with a trend for higher CD8+ T-cell abundance ($p = 0.054$) compared to the Black TNBC. No significant difference in the abundance of Treg cells ($p = 0.462$) was observed (Fig. 2D). Since the infiltration of Th1 cells and CD8+ T-cells was higher in White than Black patients, we checked the correlation of these cells with other infiltrating cells. We found that Th1 cell infiltration was significantly correlated with B-cells ($r = 0.78$, $p < 0.001$), NK cells ($r = 0.76$, $p = 0.001$) and DC infiltration ($r = 0.54$, $p = 0.046$) in Black patients, while this correlation was not present in the White patients (B-cells $r = 0.11$,

$p = 0.713$; NK cells $r = 0.14$, $p = 0.656$; DC $r = 0.18$, $p = 0.557$) (Fig. 2E). The CD8 + T-cells also showed significant positive correlation with B-cells in Black patients ($r = 0.70$, $p = 0.004$) and with NK cells in both White ($r = 0.71$, $p = 0.008$) and Black patients ($r = 0.85$, $p < 0.001$) (Fig. S2A).

In the non-TNBC samples from Black and White patients, the unsupervised hierarchical clustering created two distinct clusters, non-TNBC-Cluster 1 and 2, with relatively high and low TILs, respectively. Immune cells clustered into two major clusters, with all lymphoid origin cells being clustered in IC-Cluster 1, and TAM and DC of myeloid lineage clustering together in IC-Cluster 2. Neutrophils, NK cells, and mast cells were placed independently in IC-Cluster 3, IC-Cluster 4, and IC-Cluster 5, respectively (Fig. 3A). A slightly higher distribution (53.57%) of White non-TNBC was observed in the high TILs cluster, while the reverse was true for Black non-TNBC (48.15%) (Fig. 3B). When abundance scores for immune cell types were compared between Black and White non-TNBC, we found NK cells to be significantly higher in Black patients ($p = 0.005$), whereas DC cells were significantly lower ($p = 0.021$) in these patients, compared to the White patients (Fig. 3C). Among the T-cell subtypes, the Tregs were significantly higher ($p = 0.011$) in Black non-TNBC compared to White patients (Fig. 3D). When we compared immune cell infiltration in HR+ and HR- subtypes in Black versus White non-TNBC patients, a significantly higher infiltration of NK cells ($p = 0.003$) and Tregs ($p = 0.016$) in Black HR+ subtype was observed. Further, a trend for lower DC ($p = 0.064$) in HR+ and lower infiltration of mast cells ($p = 0.057$) and CD8+ T-cells ($p = 0.057$) in HR- subtype in Black non-TNBC were also observed as compared to their respective white non-TNBC (Fig. 3E).

TNBC tumors exhibit greater immunosuppression compared to non-TNBC tumors despite higher TILs

From a total of 770 immune-related genes in the panel, we observed differential expression of 152 genes between TNBC and non-TNBC samples, of which 122 were upregulated and 30 downregulated (Fig. 4A, B, and
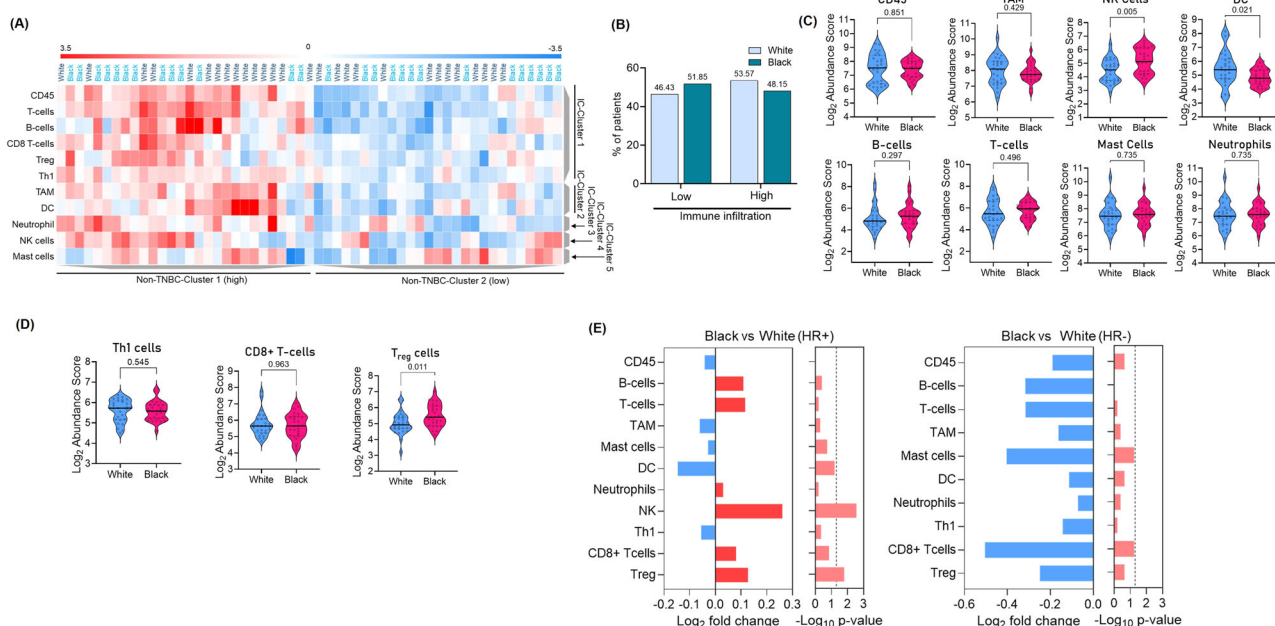

Fig. 2 | Black TNBC samples show reduced infiltration of Th1 and CD8+ T-cells.
A Heat map showing the unsupervised clustering of Black and White TNBC samples and immune cell types based on immune abundance scores in the tumor.
B Percentage distribution of Black and White TNBC samples in low and high immune infiltration clusters from the heatmap. Comparison of the immune abundance score among Black and White TNBC samples for total immune cells (CD45+), TAM, B-cells, T-cells, NK cells, 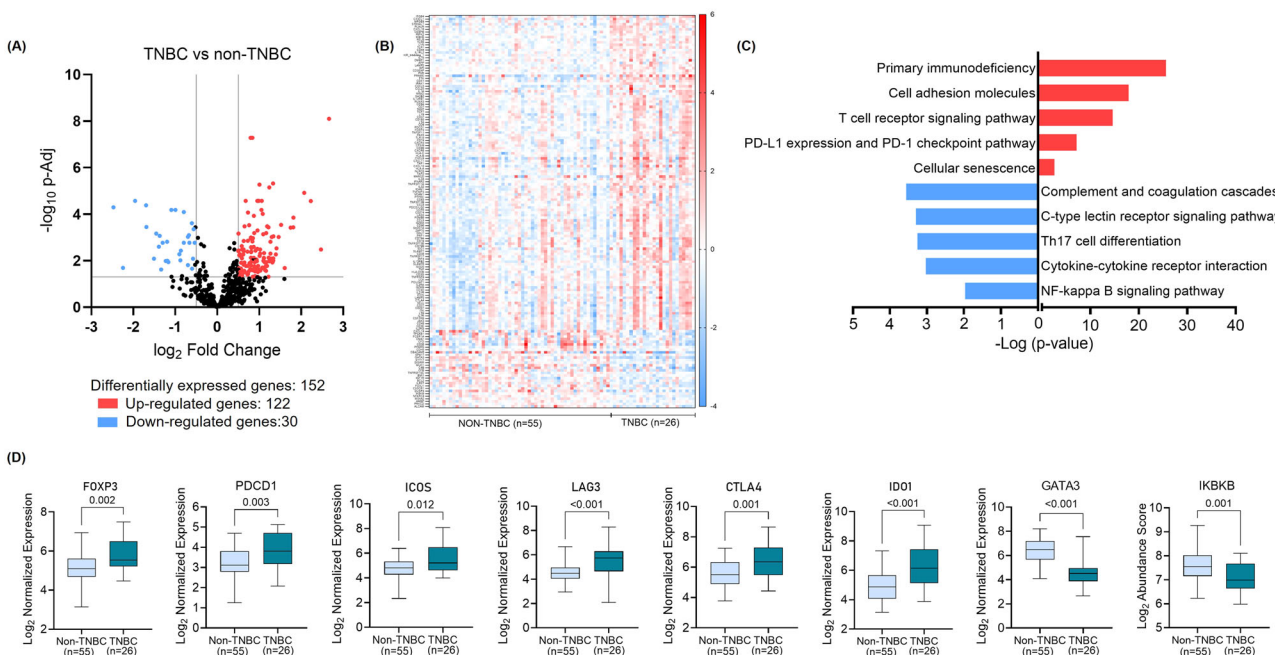neutrophils, mast cells, and DC (**C**), and in T-cells subtype cells i.e., Th1, CD8+ T-cells and Treg cells (**D**), non-parametric Mann–Whitney test was used to determine the p-value. **E** Scatter plot showing the Pearson correlation coefficient (r) for the association between infiltration of Th1 cells with B-cells, NK cells, and DC in Black and White TNBC samples; the correlation was calculated from the abundance score of immune cells in the tumor tissues. A p-value < 0.05 was considered statistically significant.

Fig. 3 | Black non-TNBC tumors have higher Treg cell infiltration. A Heat map showing the unsupervised clustering of Black and White non-TNBC samples and immune cell types based on immune abundance scores in the tumor. **B** Percentage distribution of Black and White non-TNBC samples in low and high immune infiltration clusters from the heatmap. Comparison of the immune abundance score among Black and White non-TNBC samples for total immune cells (CD45+), TAM,

NK cells, DC, B-cells, T-cells, mast cells, and neutrophils (**C**), and in T-cells subtype cells, i.e., Th1, CD8 + T-cells, and Treg cells (**D**). **E** Fold change in immune abundance score and corresponding p-values in Black samples compared to White counterpart in HR$^+$ and HR$^-$ BC subtypes. The p-value was calculated using the non-parametric Mann-Whitney test. A p-value < 0.05 was considered statistically significant.
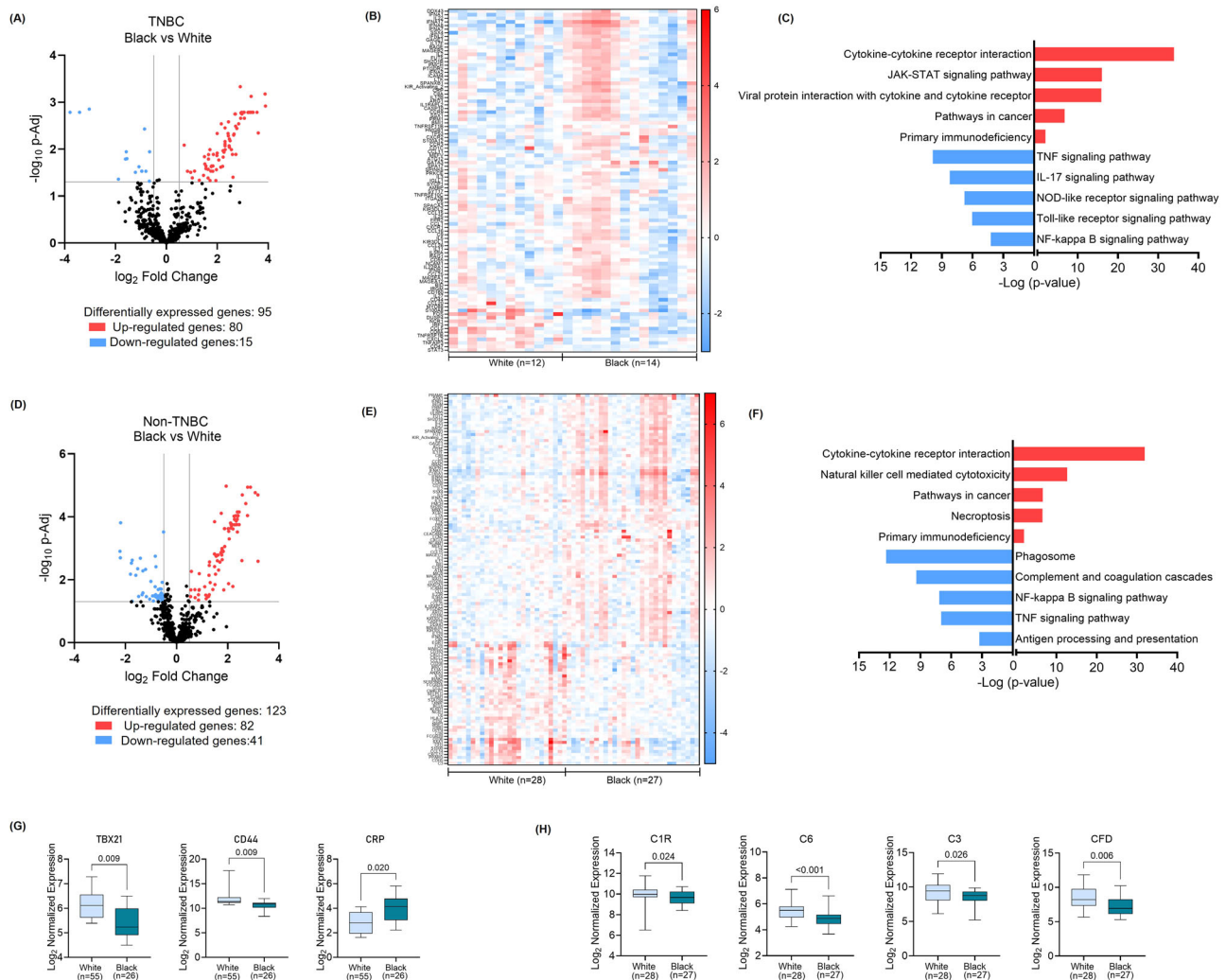

Fig. 4 | TNBC tumors exhibit greater immunosuppression than non-TNBC tumors. A Volcano plot representing the up-regulated (red dots) and down-regulated (blue dots) genes in TNBC compared to the non-TNBC samples. **B** Heat map representing the expression pattern of the differentially expressed genes among the TNBC and non-TNBC samples. **C** KEGG pathway analysis of the differentially expressed genes showing up-regulated and down-regulated pathways in TNBC

compared to non-TNBC samples. **D** Representation of selected up-regulated genes associated with immunosuppression (FOXP3, PDCD1, ICOS, LAG3, CTLA4, IDO1) and down-regulated genes associated with immune activation (GATA3, IKBKB) in TNBC compared to non-TNBC samples. The p-value was calculated using the non-parametric Mann-Whitney test. A p-value < 0.05 was considered statistically significant.

Supplementary Table S1). The KEGG pathway enrichment analysis using Enrichr web-based tool showed the primary immunodeficiency and PD-L1 expression and PD-1 checkpoint pathways to be among the top upregulated pathways in TNBC, whereas complement and coagulation cascade, c-type

signaling, and Th17 cell differentiation pathways were among the top downregulated pathways (Fig. 4C). Immunosuppressive genes such as FOXP3, PDCD1, ICOS, LAG3, CTLA4, IDO1 were significantly over-expressed in TNBC, while genes involved in immune activation such as

Fig. 5 | Black patients exhibit greater immunosuppression compared to White patients. A Volcano plot representing the up-regulated (red dots) and down-regulated (blue dots) genes in Black TNBC samples compared to the White TNBC. **B** Heat map representing the expression pattern of the differentially expressed genes among the Black and White TNBC samples. **C** KEGG pathway analysis of the differentially expressed genes showing up-regulated and down-regulated pathways in Black patients compared to White patients in TNBC. **D** Volcano plot representing the up-regulated (red dots) and down-regulated (blue dots) genes in Black non-TNBC samples compared to the White non-TNBC. **E** Heat map representing the expression pattern of 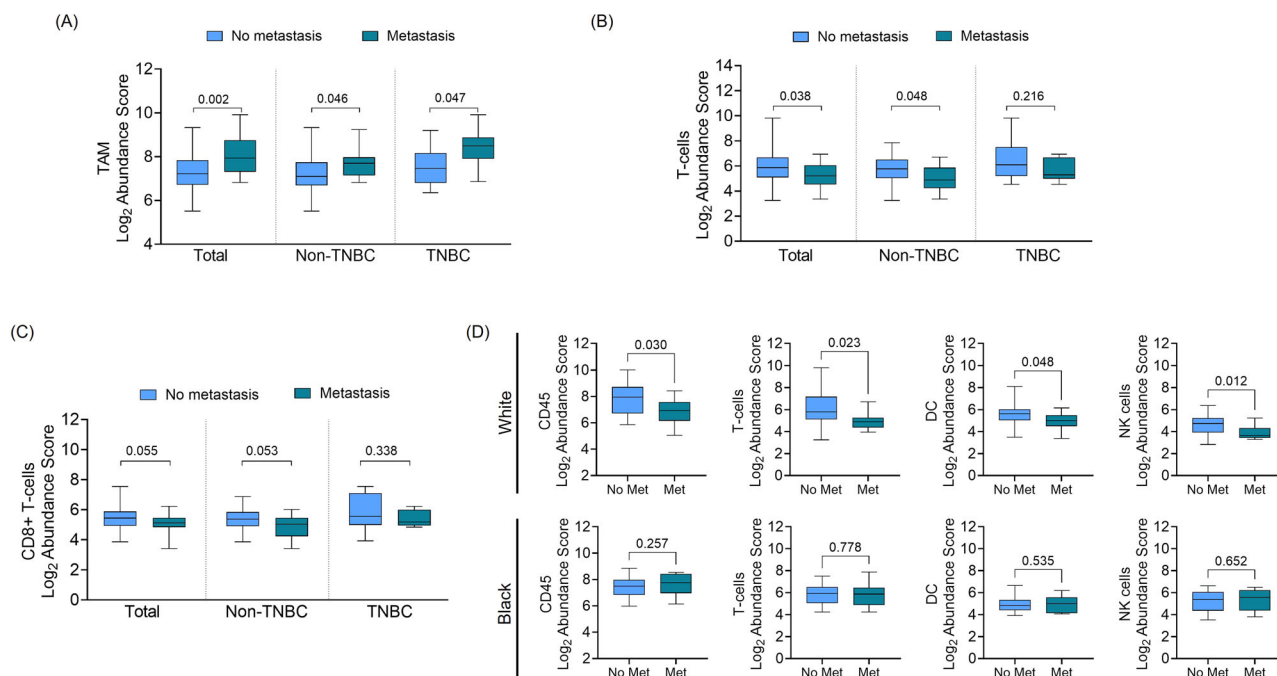the differentially expressed genes among the Black non-TNBC and White non-TNBC samples. **F** KEGG pathway analysis of the differentially expressed genes showing up-regulated and down-regulated pathways in Black patients compared to White patients in non-TNBC samples. **G** Representative genes supporting Th1 function (TBK21 and CD44) were down-regulated, and Th1 suppression (CRP) was up-regulated in Black TNBC compared to White TNBC patients. **H** Complement pathway-associated genes were down-regulated in Black non-TNBC compared to White non-TNBC patients. The p-value was calculated using the non-parametric Mann–Whitney test. A p-value < 0.05 was considered statistically significant.

GATA3 and IKBKB were significantly repressed (Fig. 4D). These findings indicate that although TNBC have relatively higher TILs than non-TNBC, they exhibit higher immunosuppression and are thus good candidate for immune checkpoint therapies.

TNBC and non-TNBC in Black patients exhibit greater immuno-suppression than in white patients

In separate race-specific comparisons within TNBC, we found a total of 95 differentially expressed genes, of which 80 were upregulated and 15 downregulated in Black patients compared to the White patients (Fig. 5A). The heatmap shows the gene expression pattern across all samples (Fig. 5B and Supplementary Table S2). The KEGG pathway enrichment analysis showed cytokine-cytokine receptor interaction, and primary immunodeficiency pathways to be among the top upregulated pathways in Black TNBC compared to White TNBC, whereas TNF, IL-17, and NOD-like receptor signaling pathways were among the top downregulated pathways (Fig. 5C).

Race-wise comparison of non-TNBC identified a total of 123 differentially-expressed genes, of which 82 were upregulated and 41 downregulated (Fig. 5D, E, and Supplementary Table S3). The pathway prediction analysis suggested upregulation of NK cell-mediated cytotoxicity and cancer and primary immunodeficiency pathways in Black patients whereas complement and coagulation cascades, NFκB signaling, and antigen processing and presentation pathways were among the top downregulated pathways in these patients (Fig. 5F). Genes regulating Th1 cells inflammatory response, TBX21 ($p = 0.009$) and Th1 cells differentiation, CD44 ($p = 0.009$), were significantly upregulated in White TNBC compared to Black TNBC, while genes involved in the suppression of Th1 differentiation, CRP ($p = 0.020$), was significantly upregulated in Black TNBC (Fig. 5G). Besides, we observed a downregulation of the complement pathway-related genes, C1R ($p = 0.024$), C6 ($p < 0.001$), C3 ($p = 0.026$), and CFD (0.005) in Black non-TNBC patients, compared to the respective subtype from white patients (Fig. 5H).

Fig. 6 | Association of immune cell abundance with BC metastasis in subtype and race. A Relative abundance of TAM in total BC, non-TNBC and TNBC samples, showing the metastatic tumors had significantly higher abundance of TAMs. **B** Relative abundance of T-cells in total BC, non-TNBC, and TNBC samples, showing the lower abundance of T-cells was significantly associated with metastasis in non-TNBC samples but not in TNBC samples. **C** Relative abundance of CD8+ T-cells in total BC, non-TNBC and TNBC samples, showing a trend for lower CD8+ T-cells abundance in non-TNBC tumors was associated with metastasis. **D** Relative abundance of total immune cells (CD45), T-cells, DC, and NK-cells in White and Black samples, showing their association with metastasis. The p-value was calculated using the non-parametric Mann–Whitney test. A p-value < 0.05 was considered statistically significant.

Race- and subtype-specific association of specific immune cell type abundance with breast cancer metastasis

Having observed race- and subtype-specific differences in the tumor immune landscape, we sought to investigate the association of the abundance of different immune cell types with BC metastasis. Our analysis revealed that metastasis-positive cases had significantly higher TAM infiltration ($p = 0.002$) in the TME in both non-TNBC ($p = 0.046$) and TNBC subtypes ($p = 0.047$) (Fig. 6A). In addition, we found that T-cell abundance was significantly lower in metastatic cases ($p = 0.038$), however, this association was significant in the non-TNBC group ($p = 0.048$) but not in TNBC ($p = 0.216$) (Fig. 6B). Further analysis of T-cell subsets indicated a strong trend for lower CD8+ T-cells in metastatic BC ($p = 0.055$), especially metastatic non-TNBC ($p = 0.053$) (Fig. 6C). In race-wise correlation, we observed that metastasis was significantly associated with the lower overall abundance of immune cells in White patients as indicated by CD45 score ($p = 0.030$). Further, in these patients, T-cells ($p = 0.023$), DC ($p = 0.048$), and NK-cells ($p = 0.012$) had a lower presence in cases with confirmed metastasis than those with non-metastatic disease. No significant association of immune cell abundance with metastatic disease was reported in Black patients (Fig. 6D).

Discussion

The type and abundance of immune cells present in the TME play a crucial role in influencing both the cancer progression and the treatment outcomes. Moreover, it could also be a good predictor for response to immune checkpoint therapies and help in treatment planning[16–18]. Immune cells normally recognize and eliminate abnormal cells, including cancer cells. However, cancer cells often develop mechanisms to evade immune detection by creating an immunosuppressive environment that reduces the efficacy of the immune response. In our study, we observed a differential immune landscape between TNBC and non-TNBC subtypes along with race-specific differences in White and Black patients. Cells of myeloid and lymphoid lineages clustered together, with some cells showing a unique clustering pattern. The infiltration of immune cells in the TME is influenced by tumor stromal composition, antigen presentation, vascularization, etc., but it is mainly regulated by chemokine secretion by cells present in the tumor[19–21]. Certain chemokines serve as chemoattractant for myeloid lineage cells, such as CCL2, CXCL2, and β-defensin, which recruit macrophages, neutrophils, and DCs, respectively[22,23], whereas CCL19, CCL21, and CXCL13 are associated with lymphoid cell (T-cells and B-cells) infiltration[24–26]. Another chemokine, CCL5, is associated with the recruitment of T-cells and NK-cells in the TME[27].

The presence and recruitment of immune cell types in the TME is also greatly influenced by the crosstalk among them[22,28,29]. We observed the highest correlation of TAM with neutrophils among the myeloid lineage cells and B-cells with T-cells among cells of the lymphoid lineage. Further, B-cells and NK cells were strongly correlated with Treg cells in TNBC, while the NK cells showed a better correlation with Th1 and CD8+ T-cells in non-TNBC, suggesting that tumor cell-intrinsic properties may also influence the crosstalk among immune cells and thus TME composition. Studies have shown that B-cells present in tumors can convert T helper cells into T regulatory cells[30,31]. Conversely, the Tregs can also suppress B-cell and NK cell function and create an immunosuppressed environment[32–35]. Thus, it is crucial to understand how these interactions vary between molecular subtypes and what their impact is on clinical outcomes.

Cancer progression as well as the outcome of immune- and chemo-therapies is influenced by the immune-active or suppressed state of the TME[36,37]. A higher presence of TILs in the TME can be indicative of a better prognosis[38,39]. However, in our study, TNBC, which has the worst prognosis[40], was found to have higher TILs in the TME. The pathway analysis of the genes differentially regulated in TNBC compared to non-TNBC suggested that the former have an immunosuppressed TME. This could likely be a reason why TNBC maintains an aggressive progression leading to its poor prognosis, despite having overall higher TILs in the TME. TNBC had a higher presence of B-cells and Tregs, which are shown to shape immunosuppressive TME[41]. It has been reported that tumors grow slower in

B-cell deficient mice exhibiting stronger Th1 and CD8+ T-cell responses[42]. Additionally, the CD40-CD40L interactions between B-cells and tumor cells derives IL-10 production leading to immunosuppression in the TME[43]. Further, the depletion of B-cells in mice model increased effectiveness of the chemotherapeutic agent oxaliplatin[44]. In humans, high B-cell infiltration in bladder, prostate, breast, and renal cancer has been linked to worse outcomes[45]. It is suggested that the antigen presentation by B-cells induces tolerogenic pathways in CD8+ T-cells, leading to anergy and impaired cytotoxic function[46–48]. The B-cells often differentiate into regulatory B-cells (Bregs) in TME, producing IL-10, IL-35, and TGFβ to suppress CD4+ Th1 and CD8+ T-cell functions[49,50]. Along these lines, earlier studies have reported the highest percentage of regulatory B-cells in TNBC, compared to other subtypes[51], and a reduced overall survival in BC patients whose tumors exhibit a higher correlative presence of Bregs and Tregs[52].

Interestingly, we observed a low abundance of the mast cells in TNBC. Their low count in the axillary lymph node is shown to be inversely proportional to the metastasis in BC patients[53], and their higher presence in tumors is associated with resistance to anti-PD-1 therapy in the humanized mouse melanoma model[54]. Combining agonistic anti-OX40 immunotherapy with mast cell blockade results in robust anti-tumor immunity in pancreatic cancer[55]. Since we observed TNBC to have low mast cells, it makes them a good candidate for immunotherapy. All the above observation aligns with clinical data of TNBC being the most aggressive and lethal breast cancer subtype, particularly in Black women. Similarly, some clinical studies have also shown a more favorable response of TNBC to immune checkpoint therapy than non-TNBC[56,57]. Since TNBC tumors have higher infiltration of Tregs and B-cells, a combined immune therapy targeting both PD-1 along with B-cell specific immune checkpoints such as TIM-1, CD40, or BTLA, could prove to be more effective in TNBC[58,59]. Therefore, analyzing specific immune cell populations can assist in precision oncology and improve the survival of BC patients.

The immune composition of TNBC varied significantly in Black and White patients and could have implications for disparate outcomes. Black TNBC had lower levels of Th1 and CD8+ T-cells in the tumor than White TNBC, along with an upregulation of immunodeficiency pathways and downregulation of immune-activating pathways. The Th1 and CD8+ T-cells promote immunity against BC cells, and higher infiltration of Th1 and CD8+ T-cells is associated with better overall survival in BC[60–62]. On the other hand, the race-wise immune landscape comparison of non-TNBC tumors showed Black patients to have higher NK and Treg cells with lower DC cells. The NK cells can directly attack and kill the cancer cells, while Treg cells can inhibit the activity of NK cells by directly interacting with them or by secreting IL-10 and TGFβ, hindering the anti-tumor immune response[63,64]. Decreased NK cell activity has been associated with higher metastasis in BC[65]. Activated DCs play a crucial role in initiating immune responses by antigen presentation to CD4+ and CD8+ T cells, which leads to the maturation and activation of tumor-specific cytotoxic T lymphocytes[66]. Lower DC infiltration in Black non-TNBC than White non-TNBC may thus cause activation of effector T-cells. The pathway analysis of the differentially expressed genes showed the immunodeficiency and PD-L1 pathway to be upregulated and the complement pathway downregulated in Black non-TNBC relative to White non-TNBC. The complement pathway stimulates the effector function of CD4+ Th1 cells and CD8+ T-cells while reducing the Treg population in tumors[67–69]. This suggests that Black non-TNBC patients have an immunosuppressed microenvironment compared to White non-TNBC patients.

We found metastatic tumors, both TNBC and non-TNBC, to have significantly higher infiltration of TAMs, which have been associated with immune suppression and tumor progression[70,71]. Conversely, T-cell abundance, particularly CD8 + T-cells, was lower in metastatic non-TNBC patients, which is often associated with poorer prognosis in cancer patients[21,72]. In White patients, metastasis was associated with lower TILs, including T-cells, DCs, and NK cells. We have recently shown that Black patients exhibit higher serum cortisol levels, and cortisol induces M2 polarization of macrophages to cause immunosuppression[73]. Other factors, including genetics and higher prevalence of obesity among Black women, could also contribute to the suppressive immune landscape and its relation to metastasis and disease prognosis[74–77].

In conclusion, this study highlights important differences in the immune landscape between TNBC and non-TNBC, as well as significant racial disparities in immune infiltration and immune activation pathways. Despite higher immune infiltration, TNBC exhibits a more immunosuppressive environment characterized by the presence of B-cells and Tregs. Race-specific differences, particularly in the abundance of key immune cell types such as T-cells, NK cells, and DCs, may contribute to disparate outcomes in Black and White patients (Fig. 7). A potential limitation of our study; however, is that all the clinical samples were procured from a single institution and thus do not have broad geographic distribution. Therefore, a future multi-institutional collaboration could not only strengthen these observations but also demonstrate if geographic and other region-specific factors (such as cultural, food choices, etc.) have an impact on the immune landscape. Moreover, although race is a social construct and socioeconomic factors play a significant role in cancer health disparities, future studies could incorporate ancestry profiling to examine if there are lineage-specific differences as well. Nonetheless, our findings highlight the importance of considering both tumor subtype and patient race when designing immune-based therapies. Further, our data suggest that targeted strategies to modulate immune cell populations, such as enhancing DC and NK cell infiltration, may be particularly beneficial in improving the response to treatment in specific racial populations.

Methods

Biospecimens
The study was conducted following the determination of "exempt" status by the Institutional Review Board (IRB). De-identified Formalin-fixed paraffin-embedded (FFPE) BC tissue blocks were obtained from the Department of Pathology, University of South Alabama. The tissue samples consisted of histologically confirmed non-TNBC ($n = 55$) and TNBC ($n = 26$) cases and were selected following H&E staining-based determination by a certified pathologist for the presence of more than 30% cancer cell area within the tumor. The description of basic characteristic features of the BC patients involved in the study is provided in Table 1. The racial classifications of the patients are based on self-reported data.

Reagents
The details of the reagents, kits, and other resources used in the study, along with their sources and catalog numbers, are provided in supplementary Table S4.
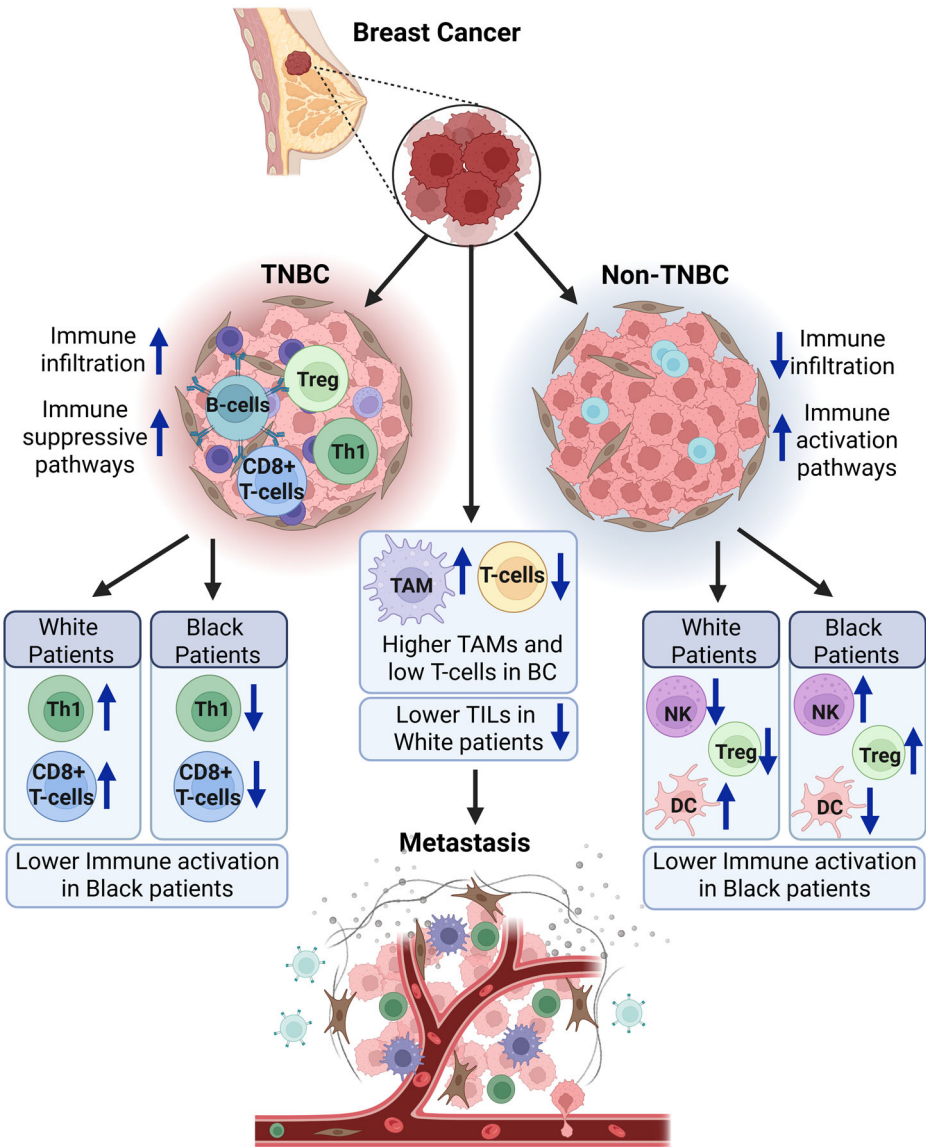
RNA isolation
FFPE tissues were sliced into 5 μm thick sections using a microtome and used for RNA isolation. The sections were collected in 1.5 ml microcentrifuge tubes, to which a deparaffination solution (Cat. No. 19093, Qiagen, MD, USA) was added. Samples were heated to 56 °C for 3 min to dissolve the paraffin, and the RNA was isolated using the RNeasy FFPE kit (Cat. No. 73504, Qiagen, MD, USA) according to the manufacturer's protocol. The quantitative and qualitative analysis of RNA was performed using a Nanodrop 1000 (Thermo Scientific, MA, USA).

Immune profiling and gene expression data
The immune profiling of the BC tissue was performed on the nanoString nCounter® pro analysis system using the PanCancer Immune Profiling Panel (nanoString Technologies, WA, USA). The RNA (150 ng in 5 μL volume) was mixed with 5 μL of hybridization buffer, 3 μL of reporter probe, and 2 μL of capture probe per sample and subjected to RNA-probe hybridization reaction for 18 h at 65 °C in a thermocycler. The hybridized samples were immobilized in the sample cartridge for imaging and counting using the nCounter Pro prep station, followed by cartridge scanning on the nCounter Pro Digital Analyzer (nanoString, WA, USA) to obtain the count data in RCC file format.

Fig. 7 | Schematic summary depicting the subtype and race-specific differences in BC immune landscape. TNBC exhibit overall higher immune cell infiltration, specifically having a greater abundance of B-cells, Tregs, Th1, and CD8+ T-cells, compared to the non-TNBC. Pathway analysis of differentially expressed genes show activation of immunosuppressive pathways despite greater immune cell infiltration. TNBC from White patients have a higher presence of Th1 and CD8+ T-cells in the TME than those from Black patients, while non-TNBC from Black patients exhibit a higher accumulation of NK and Treg cells but lower DC, compared to that in White patients. Black patients show reduced immune activation regardless of molecular subtype. Higher TAM and lower T-cell infiltration in all BC patients, and lower TILs in White patients, are indicative of the metastatic disease.

Table 1 | Characteristics of breast cancer patients

Patient cohort			
	Total patients ($n = 81$)	White ($n = 40$)	Black ($n = 41$)
Characteristics			
Age at diagnosis, range (mean)	25–85 (58.1)	25–85 (59.7)	32–83 (56.5)
Race			
White	40	N/A	N/A
Black	41	N/A	N/A
Subtype			
Non-TNBC			
HR⁺ HER2⁺/⁻	48 (59.3%)	25 (62.5%)	23 (56.1%)
HR⁻ HER2⁺	7 (8.6%)	3 (7.5%)	4 (9.8%)
TNBC			
HR⁻ HER2⁻	26 (32.1%)	12 (30%)	14 (34.1%)

In silico data analysis

The data analysis was performed using Rosalind online software. After performing the data quality check and normalization, the immune cell abundance score and differentially expressed genes for different comparisons were obtained from the Rosalind software. The unsupervised hierarchical clustering and heat maps for immune abundance in tissue samples were created using Clustergrammer online software[78]. The heat maps for differentially expressed genes were created by GraphPad Prism using the data obtained from analysis by Rosalind software. The KEGG pathway analysis of the up-regulated and down-regulated genes was performed using Enrichr[79–81] online software.

Statistical analysis

All the statistical analysis was performed using the GraphPad Prism software (GraphPad Software, CA). Statistical comparisons between two groups were performed by an unpaired, non-parametric Mann-Whitney test. The Pearson correlation coefficient was used to determine the association between immune cell type infiltration. A p-value of lower than 0.05 was considered statistically significant.

Data availability
The data that support the findings of this study are available on request from the corresponding author.

References

1. Kim, J. et al. Global patterns and trends in breast cancer incidence and mortality across 185 countries. *Nat. Med.* **31**, 1154–1162 (2025).
2. Siegel, R. L., Kratzer, T. B., Giaquinto, A. N., Sung, H. & Jemal, A. Cancer statistics, 2025. *CA Cancer J. Clin.* **75**, 10–45 (2025).
3. Eliyatkin, N., Yalcin, E., Zengel, B., Aktas, S. & Vardar, E. Molecular classification of breast carcinoma: from traditional, old-fashioned way to a new age, and a new way. *J. Breast Health* **11**, 59–66 (2015).
4. Perou, C. M. et al. Molecular portraits of human breast tumours. *Nature* **406**, 747–752 (2000).
5. Zagami, P. & Carey, L. A. Triple negative breast cancer: pitfalls and progress. *npj Breast Cancer* **8**, 95 (2022).
6. Giaquinto, A. N. et al. Breast cancer statistics 2024. *CA Cancer J. Clin.* **74**, 477–495 (2024).
7. Jatoi, I., Sung, H. & Jemal, A. The emergence of the racial disparity in U.S. breast-cancer mortality. *N. Engl. J. Med.* **386**, 2349–2352 (2022).
8. Ensenyat-Mendez, M. et al. Epigenetic profiles of triple-negative breast cancers of African American and White females. *JAMA Netw. Open* **6**, e2335821 (2023).
9. Force, U. S. P. S. T. et al. Screening for breast cancer: US preventive services task force recommendation statement. *JAMA* **331**, 1918–1930 (2024).
10. Lovejoy, L. A., Shriver, C. D., Haricharan, S. & Ellsworth, R. E. Survival disparities in US black compared to white women with hormone receptor positive-HER2 negative breast cancer. *Int. J. Environ. Res. Public Health* **20**, 2903 (2023).
11. Kumar, A., Emdad, L., Das, S. K. & Fisher, P. B. Recent advances and progress in immunotherapy of solid cancers. *Adv. Cancer Res.* **164**, 111–190 (2024).
12. Fenis, A., Demaria, O., Gauthier, L., Vivier, E. & Narni-Mancinelli, E. New immune cell engagers for cancer immunotherapy. *Nat. Rev. Immunol.* **24**, 471–486 (2024).
13. Sordo-Bahamonde, C. et al. Chemo-immunotherapy: a new trend in cancer treatment. *Cancers* **15**, 2912 (2023).
14. Sarnaik, A. A., Hwu, P., Mule, J. J. & Pilon-Thomas, S. Tumor-infiltrating lymphocytes: a new hope. *Cancer Cell* **42**, 1315–1318 (2024).
15. Harris, M. A. et al. Towards targeting the breast cancer immune microenvironment. *Nat. Rev. Cancer* **24**, 554–577 (2024).
16. Charoentong, P. et al. Pan-cancer immunogenomic analyses reveal genotype-immunophenotype relationships and predictors of response to checkpoint blockade. *Cell Rep.* **18**, 248–262 (2017).
17. Ring, B. Z., Cronister, C. T., Ring, H. Z., Ross, D. T. & Seitz, R. S. Immune infiltrate populations within distinct tumor immune microenvironments predictive of immune checkpoint treatment outcome. *Sci. Rep.* **15**, 3126 (2025).
18. Goswami, S., Pauken, K. E., Wang, L. & Sharma, P. Next-generation combination approaches for immune checkpoint therapy. *Nat. Immunol.* **25**, 2186–2199 (2024).
19. Binnewies, M. et al. Understanding the tumor immune microenvironment (TIME) for effective therapy. *Nat. Med.* **24**, 541–550 (2018).
20. Melssen, M. M., Sheybani, N. D., Leick, K. M. & Slingluff, C. L., Jr Barriers to immune cell infiltration in tumors. *J. Immunother. Cancer* **11**, e006401 (2023).
21. Yang, W. et al. T-cell infiltration and its regulatory mechanisms in cancers: insights at single-cell resolution. *J. Exp. Clin. Cancer Res.* **43**, 38 (2024).
22. Kohli, K., Pillarisetty, V. G. & Kim, T. S. Key chemokines direct migration of immune cells in solid tumors. *Cancer Gene Ther.* **29**, 10–21 (2022).
23. Schmid, M. C. & Varner, J. A. Myeloid cells in the tumor microenvironment: modulation of tumor angiogenesis and tumor inflammation. *J. Oncol.* **2010**, 201026 (2010).
24. Gowhari Shabgah, A. et al. Does CCL19 act as a double-edged sword in cancer development? *Clin. Exp. Immunol.* **207**, 164–175 (2022).
25. Rizeq, B. & Malki, M. I. The role of CCL21/CCR7 chemokine axis in breast cancer progression. *Cancers* **12**, 1036 (2020).
26. Panse, J. et al. Chemokine CXCL13 is overexpressed in the tumour tissue and in the peripheral blood of breast cancer patients. *Br. J. Cancer* **99**, 930–938 (2008).
27. Araujo, J. M. et al. Effect of CCL5 expression in the recruitment of immune cells in triple negative breast cancer. *Sci. Rep.* **8**, 4899 (2018).
28. Grivennikov, S. I., Greten, F. R. & Karin, M. Immunity, inflammation, and cancer. *Cell* **140**, 883–899 (2010).
29. Di Ceglie, I. et al. Immune cell networking in solid tumors: focus on macrophages and neutrophils. *Front. Immunol.* **15**, 1341390 (2024).
30. Olkhanud, P. B. et al. Tumor-evoked regulatory B cells promote breast cancer metastasis by converting resting CD4(+) T cells to T-regulatory cells. *Cancer Res.* **71**, 3505–3515 (2011).
31. Chien, C. H. & Chiang, B. L. Regulatory T cells induced by B cells: a novel subpopulation of regulatory T cells. *J. Biomed. Sci.* **24**, 86 (2017).
32. Gotot, J. et al. Regulatory T cells use programmed death 1 ligands to directly suppress autoreactive B cells in vivo. *Proc. Natl. Acad. Sci. USA* **109**, 10468–10473 (2012).
33. Weingartner, E. & Golding, A. Direct control of B cells by Tregs: an opportunity for long-term modulation of the humoral response. *Cell Immunol.* **318**, 8–16 (2017).
34. Ghiringhelli, F. et al. CD4+CD25+ regulatory T cells inhibit natural killer cell functions in a transforming growth factor-beta-dependent manner. *J. Exp. Med.* **202**, 1075–1085 (2005).
35. Liu, W. et al. CCR4 mediated chemotaxis of regulatory T cells suppress the activation of T cells and NK cells via TGF-beta pathway in human non-small cell lung cancer. *Biochem. Biophys. Res. Commun.* **488**, 196–203 (2017).
36. Mao, X. et al. Crosstalk between cancer-associated fibroblasts and immune cells in the tumor microenvironment: new findings and future perspectives. *Mol. Cancer* **20**, 131 (2021).
37. Otterlei Fjortoft, M., Huse, K. & Rye, I. H. The tumor immune microenvironment in breast cancer progression. *Acta Oncol.* **63**, 359–367 (2024).
38. Denkert, C. et al. Tumour-infiltrating lymphocytes and prognosis in different subtypes of breast cancer: a pooled analysis of 3771 patients treated with neoadjuvant therapy. *Lancet Oncol.* **19**, 40–50 (2018).
39. Wang, K., Xu, J., Zhang, T. & Xue, D. Tumor-infiltrating lymphocytes in breast cancer predict the response to chemotherapy and survival outcome: a meta-analysis. *Oncotarget* **7**, 44288–44298 (2016).
40. Hwang, K. T. et al. Impact of breast cancer subtypes on prognosis of women with operable invasive breast cancer: a population-based study using SEER database. *Clin. Cancer Res.* **25**, 1970–1979 (2019).
41. Hanahan, D. & Weinberg, R. A. Hallmarks of cancer: the next generation. *Cell* **144**, 646–674 (2011).
42. Shah, S. et al. Increased rejection of primary tumors in mice lacking B cells: inhibition of anti-tumor CTL and TH1 cytokine responses by B cells. *Int. J. Cancer* **117**, 574–586 (2005).

43. Inoue, S., Leitner, W. W., Golding, B. & Scott, D. Inhibitory effects of B cells on antitumor immunity. *Cancer Res.* **66**, 7741–7747 (2006).

44. Kroemer, G., Galluzzi, L., Kepp, O. & Zitvogel, L. Immunogenic cell death in cancer therapy. *Annu. Rev. Immunol.* **31**, 51–72 (2013).

45. Sharonov, G. V., Serebrovskaya, E. O., Yuzhakova, D. V., Britanova, O. V. & Chudakov, D. M. B cells, plasma cells and antibody repertoires in the tumour microenvironment. *Nat. Rev. Immunol.* **20**, 294–307 (2020).

46. Van Meerhaeghe, T., Neel, A., Brouard, S. & Degauque, N. Regulation of CD8 T cell by B-cells: a narrative review. *Front. Immunol.* **14**, 1125605 (2023).

47. Bennett, S. R., Carbone, F. R., Toy, T., Miller, J. F. & Heath, W. R. B cells directly tolerize CD8(+) T cells. *J. Exp. Med.* **188**, 1977–1983 (1998).

48. Hollsberg, P., Batra, V., Dressel, A. & Hafler, D. A. Induction of anergy in CD8 T cells by B cell presentation of antigen. *J. Immunol.* **157**, 5269–5276 (1996).

49. Rosser, E. C. & Mauri, C. Regulatory B cells: origin, phenotype, and function. *Immunity* **42**, 607–612 (2015).

50. Chen, K. X., Gresh, N. & Pullman, B. Groove selectivity in the interaction of 9-aminoacridine-4-carboxamide antitumor agents with DNA. *FEBS Lett.* **224**, 361–364 (1987).

51. Li, R. & Cao, L. The role of tumor-infiltrating lymphocytes in triple-negative breast cancer and the research progress of adoptive cell therapy. *Front. Immunol.* **14**, 1194020 (2023).

52. Steenbruggen, T. G. et al. B-cells and regulatory T-cells in the microenvironment of HER2+ breast cancer are associated with decreased survival: a real-world analysis of women with HER2+ metastatic breast cancer. *Breast Cancer Res.* **25**, 117 (2023).

53. Naik, R., Baliga, P., Bansal, R. & Pai, M. Distribution of mast cells in the axillary lymph nodes of breast cancer patients. *J. Indian Med. Assoc.* **95**, 606–607 (1997).

54. Somasundaram, R. et al. Tumor-infiltrating mast cells are associated with resistance to anti-PD-1 therapy. *Nat. Commun.* **12**, 346 (2021).

55. Ma, Y. et al. Tumor-infiltrating mast cells confer resistance to immunotherapy in pancreatic cancer. *iScience* **27**, 111085 (2024).

56. Schmid, P. et al. Pembrolizumab for early triple-negative breast cancer. *N. Engl. J. Med.* **382**, 810–821 (2020).

57. Brown, S. R. & Vomhof-DeKrey, E. E. Current immunotherapy treatments of primary breast cancer subtypes. *Biomedicines* **12**, 895 (2024).

58. Flippot, R. et al. B cells and the coordination of immune checkpoint inhibitor response in patients with solid tumors. *J. Immunother. Cancer* **12**, e008636 (2024).

59. Stefanski, A. L. & Dorner, T. Immune checkpoints and the multiple faces of B cells in systemic lupus erythematosus. *Curr. Opin. Rheumatol.* **33**, 592–597 (2021).

60. Noel, G. et al. Functional Th1-oriented T follicular helper cells that infiltrate human breast cancer promote effective adaptive immunity. *J. Clin. Investig.* **131**, e139905 (2021).

61. Xiao, Y., Huang, Y., Jiang, J., Chen, Y. & Wei, C. Identification of the prognostic value of Th1/Th2 ratio and a novel prognostic signature in basal-like breast cancer. *Hereditas* **160**, 2 (2023).

62. Oshi, M. et al. CD8 T cell score as a prognostic biomarker for triple negative breast cancer. *Int. J. Mol. Sci.* **21**, 6968 (2020).

63. Chan, I. S. & Ewald, A. J. The changing role of natural killer cells in cancer metastasis. *J. Clin. Investig.* **132**, e143762 (2022).

64. Cozar, B. et al. Tumor-infiltrating natural killer cells. *Cancer Discov.* **11**, 34–44 (2021).

65. Bottos, A. et al. Decreased NK-cell tumour immunosurveillance consequent to JAK inhibition enhances metastasis in breast cancer models. *Nat. Commun.* **7**, 12258 (2016).

66. Retecki, K., Seweryn, M., Graczyk-Jarzynka, A. & Bajor, M. The immune landscape of breast cancer: strategies for overcoming immunotherapy resistance. *Cancers* **13**, 6012 (2021).

67. Arbore, G. et al. Complement receptor CD46 co-stimulates optimal human CD8(+) T cell effector function via fatty acid metabolism. *Nat. Commun.* **9**, 4186 (2018).

68. Gadwa, J. et al. Complement C3a and C5a receptor blockade modulates regulatory T cell conversion in head and neck cancer. *J. Immunother. Cancer* **9**, e002585 (2021).

69. Kwan, W. H., van der Touw, W., Paz-Artal, E., Li, M. O. & Heeger, P. S. Signaling through C5a receptor and C3a receptor diminishes function of murine natural regulatory T cells. *J. Exp. Med.* **210**, 257–268 (2013).

70. Su, P. et al. Targeting tumor-associated macrophages: critical players in tumor progression and therapeutic strategies (Review). *Int. J. Oncol.* **64**, 60 (2024).

71. Padzinska-Pruszynska, I. et al. Macrophages: key players in the battle against triple-negative breast cancer. *Int. J. Mol. Sci.* **25**, 10781 (2024).

72. Sun, Y. P., Ke, Y. L. & Li, X. Prognostic value of CD8(+) tumor-infiltrating T cells in patients with breast cancer: a systematic review and meta-analysis. *Oncol. Lett.* **25**, 39 (2023).

73. Sharma, A. et al. Cortisol affects macrophage polarization by inducing miR-143/145 cluster to reprogram glucose metabolism and by promoting TCA cycle anaplerosis. *J. Biol. Chem.* **300**, 107753 (2024).

74. Thomas, C. E. & Peters, U. Genomic landscape of cancer in racially and ethnically diverse populations. *Nat. Rev. Genet.* **26**, 336–349 (2024).

75. Parab, A. Z. et al. Socioecologic factors and racial differences in breast cancer multigene prognostic scores in US Women. *JAMA Netw. Open* **7**, e244862 (2024).

76. Zavala, V. A. et al. Cancer health disparities in racial/ethnic minorities in the United States. *Br. J. Cancer* **124**, 315–332 (2021).

77. Sudan, S. K. et al. Obesity and early-onset breast cancer and specific molecular subtype diagnosis in black and white women: NIMHD Social Epigenomics Program. *JAMA Netw. Open* **7**, e2421846 (2024).

78. Fernandez, N. F. et al. Clustergrammer, a web-based heatmap visualization and analysis tool for high-dimensional biological data. *Sci. Data* **4**, 170151 (2017).

79. Chen, E. Y. et al. Enrichr: interactive and collaborative HTML5 gene list enrichment analysis tool. *BMC Bioinform.* **14**, 128 (2013).

80. Kuleshov, M. V. et al. Enrichr: a comprehensive gene set enrichment analysis web server 2016 update. *Nucleic Acids Res.* **44**, W90–W97 (2016).

81. Xie, Z. et al. Gene set knowledge discovery with Enrichr. *Curr. Protoc.* **1**, e90 (2021).

Acknowledgements

Author contributions

S.S. conceptualized the idea of this study. S.S. and A.P.S. designed the experimental plan and supervised the study. A.S., S.K.S., K.S.V., and M.A.K. performed the experiments, analyzed, and interpreted the data. M.T. reviewed the slides and assisted in the pathological examination of clinical specimens. S.S., J.E.C., and T.K. procured the specimens. C.N. collected the sample information. S.S. and A.P.S. obtained additional resources and helped in data interpretation and presentation. S.S. obtained funding. A.S. coordinated with all the team members, prepared all the figures, and wrote the first manuscript draft and incorporated any revisions. All the authors reviewed the manuscript.

Competing interests

The authors declare no competing interests.

Additional information

Supplementary information The online version contains supplementary material available at https://doi.org/10.1038/s41523-025-00799-8.

Correspondence and requests for materials should be addressed to Seema Singh.

Reprints and permissions information is available at http://www.nature.com/reprints

Publisher's note Springer Nature remains neutral with regard to jurisdictional claims in published maps and institutional affiliations.